Geomechanics and Engineering, *Vol. 41, No. 2 (2025) 177-187*
https://doi.org/10.12989/gae.2025.41.2.177

Dynamic properties of well-graded sand with silt

Nuraiym Paiyz[a], Sung-Woo Moon*, Alfrendo Satyanaga[b] and Jong Kim[c]

Department of Civil and Environmental Engineering, School of Engineering and Digital Sciences
Nazarbayev University, 53, Kabanbay batyr Ave., Astana, 010000, Republic of Kazakhstan

(*Received December 4, 2024, Revised March 5, 2025, Accepted March 18, 2025*)

Abstract. Understanding the dynamic properties of soils—particularly their behavior under cyclic or dynamic loading conditions, such as those induced by seismic events or construction activities—is critical for designing resilient geotechnical structures and foundations. This study investigates well-graded sand with silt soils from Astana, Kazakhstan, using the Resonant Column (RC) and Cyclic Torsional Shear (CTS) tests, to characterize their dynamic behavior under varying confining pressures (σ_c). Although seismic activity in Astana is generally low, aftershocks from distant earthquakes highlight the importance of understanding site-specific seismic risks. This study provides site-specific shear modulus reduction (G) and material damping ratio (D) curves, essential for evaluating seismic hazards and mitigating disasters. These findings address significant gaps in the dynamic characterization of well-graded sand with silt and have practical applications in seismic risk mitigation, foundation design, and urban planning, contributing to safer and more resilient infrastructure in earthquake-prone regions.

Keywords: cyclic torsional shear testing; damping ratio; dynamic soil characterization; resonant column apparatus; shear modulus; well-graded sand with a silt

1. Introduction

Ensuring the safety and stability of foundations and buildings requires a comprehensive understanding under diverse stress scenarios, such as those induced by construction activities or seismic events. Soil liquefaction - a phenomenon that weakens the soil and compromises structural integrity - can lead to road distortions, building tilting, and bridge collapses (Moon *et al.* 2024). This underscores the importance of accurately assessing the dynamic response of liquefaction-prone sites to guide appropriate mitigation strategies.

Engineers can select the most effective soil improvement techniques by comparing the treated site's dynamic response with that of untreated soil (Khoshemehr and Bahadori 2023). Addressing geotechnical challenges, such as liquefaction susceptibility, is a critical prerequisite before commencing construction, especially in seismic zones. Such risks necessitate a profound understanding of dynamic soil properties, which are essential for geotechnical applications, including probabilistic seismic hazard assessment (PSHA) and the design of resilient foundation systems.

Determining the dynamic characteristics of the soils is crucial when building structures in seismically active zones. To minimize potential damage, the soil's response under cyclic and sustained loads should be thoroughly understood and integrated into design considerations (Güler and Afacan 2023, Cui *et al.* 2023). By doing so, geotechnical engineers can develop strategies to enhance soil performance, ensuring the stability and longevity of structures in earthquake-prone areas.

Dynamic soil characteristics are typically investigated using a combination of laboratory and field-testing techniques. Field methods include seismic refraction, reflection, and multi-channel analysis of surface waves (MASW), which provide critical insights into soil behavior under dynamic conditions (Abdialim *et al.* 2024). Complementing these, laboratory techniques such as resonant column tests, bender elements, cyclic triaxial, and torsional tests offer controlled environments to study soil response at various strain levels.

Among laboratory methods, the resonant column apparatus (RCA) is particularly effective for evaluating dynamic soil properties across a narrow strain range. In RCA testing, a cylindrical soil specimen is vibrated in torsional or flexural modes, enabling accurate measurement of key parameters such as shear modulus (G), material damping (D), and shear strain (Sas *et al.* 2017). By examining these properties under varying confining pressures (σ_c) and strain amplitudes, RCA testing provides valuable insights into factors affecting soil stiffness and damping behavior.

Despite its effectiveness, limited research has explored the dynamic soil properties of Kazakhstan, particularly Astana. Approximately 25% of Kazakhstan's land is seismically active, with the highest risks concentrated in the South, Southeast, and East (Zhanabayeva *et al.* 2023). Although Astana experiences low seismic activity, aftershocks from distant earthquakes in China and Kyrgyzstan have been felt, underscoring the importance of

*Corresponding author, Associate Professor
E-mail: sung.moon@nu.edu.kz
[a]Graduate Student
[b]Associate Professor
[c]Professor

ISSN: 2005-307X (Print), 2092-6219 (Online)

evaluating the city's seismic hazards. Additionally, residential structures built before the 1990s lack modern earthquake-resistant features, making them particularly vulnerable (Rashid *et al.* 2023).

Kazakhstan's seismic design framework has evolved significantly over the past 50 years, transitioning from Soviet-based standards to updated building codes, such as the SNiP regulations revised in 1998 to incorporate advancements in global earthquake engineering research (Zhanabayeva *et al.* 2023). Nonetheless, thorough site-specific soil characterization remains essential, especially in areas susceptible to seismic activity.

This study addresses these challenges by employing the resonant column apparatus (RCA) and advanced soil testing techniques to investigate the dynamic properties of well-graded sand with silt soils from Astana. The primary objective is to assess shear modulus reduction curves and material damping ratio (D) curves, which are essential for improving seismic risk assessment and enhancing the regional preparedness for seismic events.

The novelty of the study lies in bridging critical gaps in existing knowledge. To date, the dynamic properties of soils in Kazakhstan have not been extensively investigated using RCA, particularly for well-graded sand with silt soils. In addition, this study marks the first application of RCA in this region to evaluate soil behavior under dynamic conditions. By addressing these gaps, the research advances geotechnical understanding both locally and globally.

The findings have practical implications for engineering practices. The shear modulus reduction curves and material damping ratio (D) curves developed in this study provide essential data for seismic risk assessments, foundation design, and urban planning. Integrating these dynamic properties into local seismic design codes will improve the resilience of critical infrastructure and guide the development of earthquake-resistant buildings, especially in rapidly urbanizing regions.

Furthermore, the study's insights into soil behavior under dynamic loads can inform urban planning strategies, such as zoning and site selection, to mitigate seismic risks in vulnerable areas. These contributions reinforce the importance of geotechnical research in guiding sustainable and resilient urban development.

2. Test material

The soil samples for this study were collected from an active construction site in Astana, Kazakhstan. The near-surface layer was identified as well-graded sand with silt, with a maximum dry density (MDD) of 1.868 kN/m3 and an optimum moisture content (OMC) of 14.0%, determined by the standard compaction test. According to the Unified Soil Classification System (ASTM D2487), the soil is classified as well-graded sand with silt (SW-SM). Table 1 summarizes the key index properties, including dry bulk density, liquid limit (LL), plastic limit (PL), and plasticity index (PI), which indicate very low plasticity – a

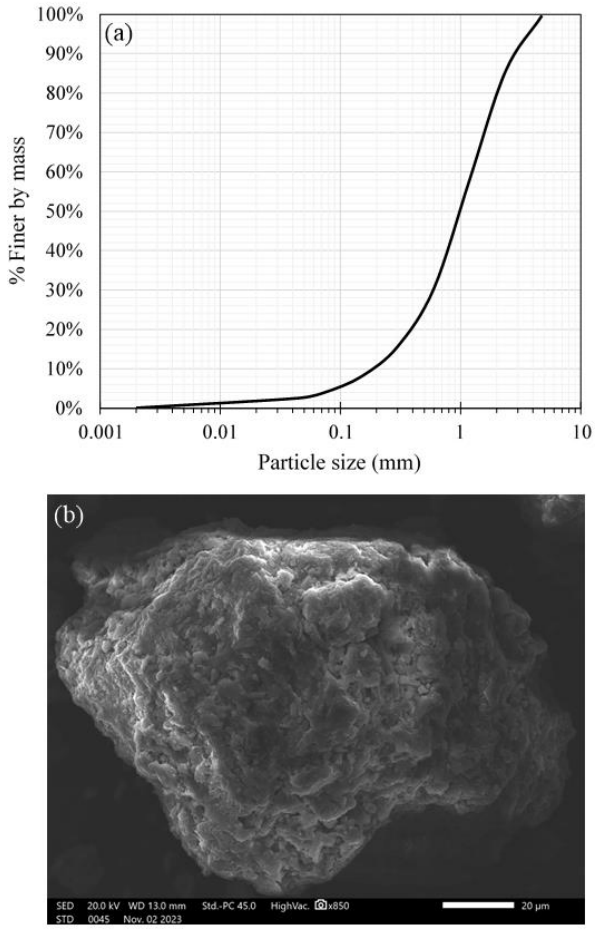

Fig. 1 Properties of the tested soil: (a) Particle size distribution curve, (b) SEM image

characteristic common in sandy soils with fines. The LL and PL of the tested material were determined in accordance with ASTM D4318. Given the low fine content (5%), the standard procedure was modified by conducting multiple trials to ensure measurement consistency, minimize variability, and improve result reliability. This approach was essential to mitigate the potential impact of low clay activity and limited cohesion, which can affect the precision of Atterberg limit determinations in coarse-grained soils.

Scanning electron microscopy (SEM) was employed to obtain high-resolution images of the sand particles, revealing their sub-angular shape. Fig. 1 illustrates this morphology, which is typical of sand found in environments with minimal transport, such as construction sites or newly exposed deposits. According to previous studies, particle shape significantly influences the collapse and settlement behavior of soil under shearing and wetting conditions (Mahinroosta and Oshtaghi 2021). The particle size distribution curve, presented in Fig. 1, and the gradation parameters (Table 1) further characterize the well-graded sand with silt.

The chemical composition of the soil highlights a complex mineral makeup with both major and minor constituents. The primary components include silicon

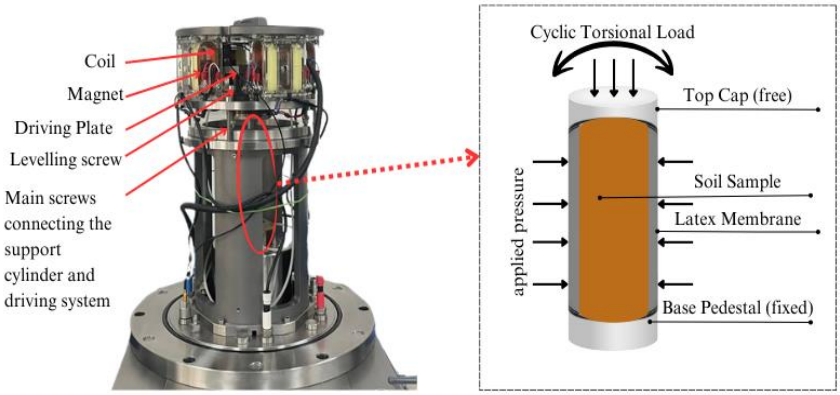

Fig. 2 Resonant Column Apparatus (RCA) with its components and sample testing conditions

Table 1 Physical characteristics of the soil specimen

Type of sand	Well-graded sand
USCS classification	SW-SM
Liquid limit (LL)	32
Plastic limit (PL)	22
Plasticity index (PI)	10
Dry bulk density (ρ, Mg/m^3)	1.4
D10 (mm)	0.3
D30 (mm)	0.95
D60 (mm)	2
Uniformity coefficient, C_u	6.7
Coefficient of curvature, C_c	1.5

dioxide (SiO_2) at 42.06%, iron oxide (FeO_3) at 21.16%, and aluminum oxide (AlO_3) at 12.35%, indicating the soil's high quartz content – hallmark of sandy soils. The presence of AlO_3 and FeO_3 suggests contributions from clay minerals and iron compounds, which enhance the soil's cohesive properties.

Minor components include Sulfur Trioxide (SO_3), Calcium Oxide (CaO), Potassium Oxide (K_2O), Titanium Dioxide (TiO_2), and Magnesium Oxide (MgO). While present in smaller quantities, these constituents may influence the soil's chemical reactivity and durability under various environmental conditions.

3. Methodology

3.1 Sample preparation

Several methods for sample preparation, including spooning, raining, wet tamping, moist vibration, and air pluviation, have been proposed for geotechnical testing (Ishihara *et al.* 1978). The selection of a preparation method is critical as factors such as sample preparation and testing procedures significantly influence soil strength (Silver *et al.* 1980). Previous studies have shown that cyclic strength is affected by variations in specimen dimensions; for instance, specimens with a diameter (d) of 300 mm exhibited approximately 10% lower strength compared to those with d = 70 mm (Wong *et al.* 1975). Based on these findings, a sample size of 70 mm in diameter and 140 mm in height was chosen for this study.

Soil samples were collected from the Astana construction site and carefully prepared to preserve their original composition and structure, which is essential for reliable testing. The samples, classified as well-graded sand with silt, were compacted to maintain their MDD and OMC of 14.0%, ensuring the accuracy and consistency of the subsequent testing results. Proper labeling, categorization, and regulated storage were implemented to prevent contamination or alterations to the samples.

The sample preparation process followed the standards outlined in ASTM D4015 (2014) to ensure compliance with established guidelines. This involved forming the samples into consistent sizes required for the dynamic soil property tests. Maintaining the original density and moisture content throughout the preparation process was critical to accurately simulate field conditions. By adhering to these procedures, the preparation process enhanced the precision of dynamic soil property testing, enabling a comprehensive understanding of soil behavior under various loading conditions.

3.2 Experimental setup

The resonant column apparatus (RCA) is a widely used tool for evaluating dynamic soil properties, capable of performing both resonant and cyclic torsional shear tests. It applies small cyclic torsional forces to a prepared soil specimen through an electromagnetic mechanism. Dynamic parameters, such as shear modulus (G), shear wave velocity (V_s), and damping ratio (D), are calculated by measuring the soil's response with an accelerometer and adjusting the loading frequency to match the resonance frequency (Sakshi and Sebastian 2023). This method allows for the detailed analysis of soil behavior under varying confining pressures and strain levels, typically ranging from 10^{-5} to 10^{-2} %.

For this study, the RCA from GDS Instruments was utilized to investigate the effects of confining pressures (50–200 kPa) on well-graded sand with silt from Astana. As shown in Fig. 2, the fixed-free configuration of the RCA was selected as the

Table 2 Results of the calibration of the drive system

		f_n*(Hz)	ω(rad/s)	ω^2(rad/s)^2	$1/\omega^2 \cdot 10^{-6}$ (1/rad^2)	I_0, Intercept
15 mm bar	Top plate	73.5	461.814	213272.3	4.689	-0.004009087
	Weight #1	72.1	453.017	205225	4.873	
	Weight #2	71.2	447.362	200133.5	4.997	
	Weight #3	70.6	443.592	196774.6	5.082	
12.5 mm bar	Top plate	52.2	327.983	107572.4	9.296	-0.003370528
	Weight #1	51.5	323.584	104706.6	9.55	
	Weight #2	50.2	315.416	99487.2	1.055	
	Weight #3	50.1	314.788	99091.2	1.009	
10 mm bar	Top plate	33.8	212.372	45101.7	2.217	-0.00384692
	Weight #1	33.3	209.231	43777.2	2.284	
	Weight #2	32.8	206.088	42472.5	2.354	
	Weight #3	32.4	203.575	41442.9	2.413	
Average						-0.003742178

*f_n – resonant frequency of the calibration bar; ω-natural circular frequency of vibration of the sample

most suitable setup, as it allows for the application of sinusoidal torque via an electromagnetic drive mechanism. The setup includes a four-arm rotor equipped with magnets and wire coils securely attached to the soil sample.

During testing, the height of the supporting cylinder was carefully adjusted to center the magnets within the coils, ensuring precise and consistent results. The RCA's fixed-free configuration allowed for accurate measurement of dynamic soil properties across a range of strain amplitudes and confining pressures. A typical resonant frequency graph generated during testing is shown in Fig. 3, highlighting the soil's response and resonance characteristics under controlled conditions.

The RCA system offers several design enhancements to improve measurement accuracy. For instance, the device minimizes errors caused by equipment damping, as the movement of magnets in the coils during free vibration decay generates an opposing electromagnetic field, reducing measurement inaccuracies (Szilvágyi 2018). Additionally, the RCA features stiff connections between coils and the base plate, enclosed within a Perspex jacket, which ensures structural stability and precision. These improvements, combined with the ability to simulate realistic cyclic loading conditions, make the RCA an ideal tool for studying the dynamic behavior of well-graded sand with silt.

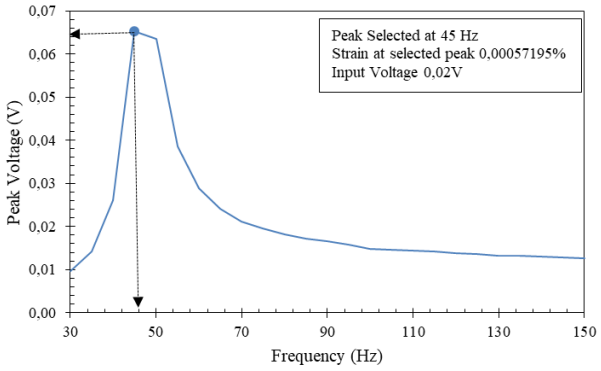

Fig. 3 A common representation of the resonance frequency at a specific amplitude of shear strain

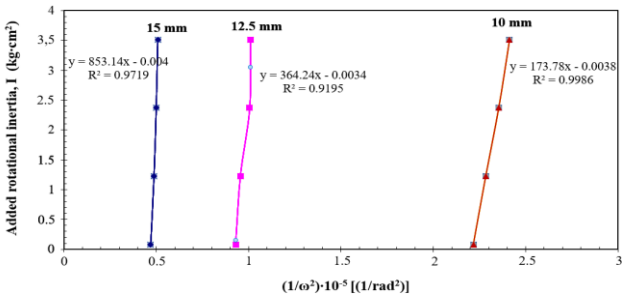

Fig. 4 Calibration results using added masses for aluminum bars for varying diameter

3.3 Testing procedure

3.3.1 Calibration procedure

To accurately compute the mass polar moment of inertia (I_0) and moment of inertia (I_y) of the resonant column drive system, a calibration procedure was conducted using aluminum calibration bars of known stiffness. This calibration was performed in compliance with ASTM D4015 (2015) by replacing the test specimen with metal bars whose mechanical properties were pre-established.

The test involved running three trials for each aluminum bar under varying calibration weights attached to the drive system. For each trial, the resonance frequency and peak amplitude were recorded at a specified input voltage (Shinde and Kumar 2021). The resonant frequencies for aluminum specimens were observed to range from 32.4 Hz to 73.5 Hz (Table 2).

As shown in Table 2, the resonant frequency increases with the bar diameter. Using the calibration results, the mass polar

Table 3 Calculated values for shear modulus determination

Parameter	Value
I_0 (m)	-0.003742178
I (m)	0.00042875
I/I_0	-0.114571642
β	0.10469
Dry bulk density (ρ, Mg/m^3)	1.4

moment of inertia of the added mass (I_{am}) was plotted against $1/\omega^2$, and a straight line was generated with k as the gradient and I_0 as the intercept (Fig. 4).

Establishing the shear modulus (G) of the soil samples requires precise determination of I_0. Since I_0 is frequency-dependent, it is calculated over the entire frequency range for the soil being tested. The shear wave velocity (V_s) is computed before determining the shear modulus (G) using the following equation

$$V_s = \frac{2\pi f L}{\beta} \quad (1)$$

where, f is the resonant frequency, L is the sample length, β is determined using Eq. (2)

$$\frac{I}{I_0} = \beta \cdot \tan(\beta) \quad (2)$$

The value of I_0 was determined from calibration to be -0.00374 (Table 2). The mass polar moment of inertia of the sample (I) is calculated as

$$I = \frac{md^2}{8} \quad (3)$$

Finally, the shear modulus (G) is is calculated using the following formula, with values derived from Table 3

$$G = \rho \cdot v_s^2 \quad (4)$$

3.3.2 Main procedure

Data acquisition for the cyclic torsional shear (CTS), damping, and resonant column (RC) tests was performed using the GDSLab and GDSRCA software. Prior to testing, the specimen underwent saturation and consolidation following a detailed procedure. The preparation began with thorough cleaning of the testing equipment to remove any residue that might affect accuracy. De-aired water was then introduced into the pore pressure mechanism to eliminate air gaps and ensure a bubble-free system. To facilitate efficient water distribution throughout the system during the consolidation process, filter papers were placed on the top and bottom surfaces of the soil specimen.

The soil specimen was encapsulated within two latex membranes to prevent air infiltration. It was then placed in the testing cell for saturation using the back-pressure technique. In this process, the cell pressure and back pressure were gradually increased until Skempton's B-value exceeded 0.95 (Sas *et al.* 2017). This ensured that the well-graded sand with silt specimen was fully saturated, with all air removed from the intergranular spaces.

Following saturation, the consolidation process commenced at a confining pressure (σ_c) of 50 kPa. This step was maintained for a duration of 24 to 48 hours, allowing the sample to reach equilibrium under controlled conditions (Flores-Guzmán *et al*. 2014). Once the first consolidation stage was completed, data collection began for RC, damping, and CTS tests.

The consolidation step is critical for understanding how the soil responds to applied loads, particularly in terms of long-term settlement behavior. Meanwhile, the saturation process ensures that the specimen replicates field conditions by maintaining a fully saturated state (B-value > 0.95). This approach provides highly reliable data for dynamic soil behavior under various engineering applications.

For resonant column testing, the RC controller generated a sine wave signal with a predetermined amplitude. This signal was enhanced by a power amplifier and transmitted to the resonant column unit, where it was evenly distributed across four electromagnetic coils. The resulting torque caused the soil specimen to vibrate. The vibration response of the specimen was recorded by an accelerometer, and the resulting signal was sent to a charge amplifier, which transmitted the data to the controller. The software processed the results, displaying amplitude as a function of frequency.

The RC test was repeated at confining pressures (σ_c) of 100, 150, and 200 kPa to evaluate the dynamic response of the soil specimen under varying conditions. This procedure provided critical data on the soil's behavior during CTS, damping, and RC tests, enabling a comprehensive analysis of its dynamic properties.

After deriving data from RC testing, CTS testing was conducted on the same apparatus. Similar to RC testing, CTS tests were performed by gradually increasing the excitation voltage, starting from the lowest feasible value and reaching up to 1%. The CTS test involves ten cycles of cyclic torsional vibration with a low frequency (0.5 Hz) along the test specimen's vertical axis (Sakshi and Sebastian 2023). To perform the CTS tests, the specimen was first excited using the lowest feasible excitation voltage. Following the initial stimulation, the voltage was progressively raised across a range of strain levels until it reached 1% for subsequent testing.

4. Results and discussion

4.1 Resonant column (RC) testing

Resonant column testing (RCT) is a well-established method for accurately assessing soil stiffness and damping properties at low-to-medium shear strain levels, typically ranging from 0.0001% to 0.01%. Originally developed by Iida in 1938, the technique has been refined over decades, with significant contributions from researchers such as Hardin and Music (1965) and Hardin (1970). The method has since been standardized under ASTM D 4015-92 (2015) (Clayton *et al.* 2009).

The fundamental principle of RC testing involves vibrating a cylindrical soil sample in its basic mode of

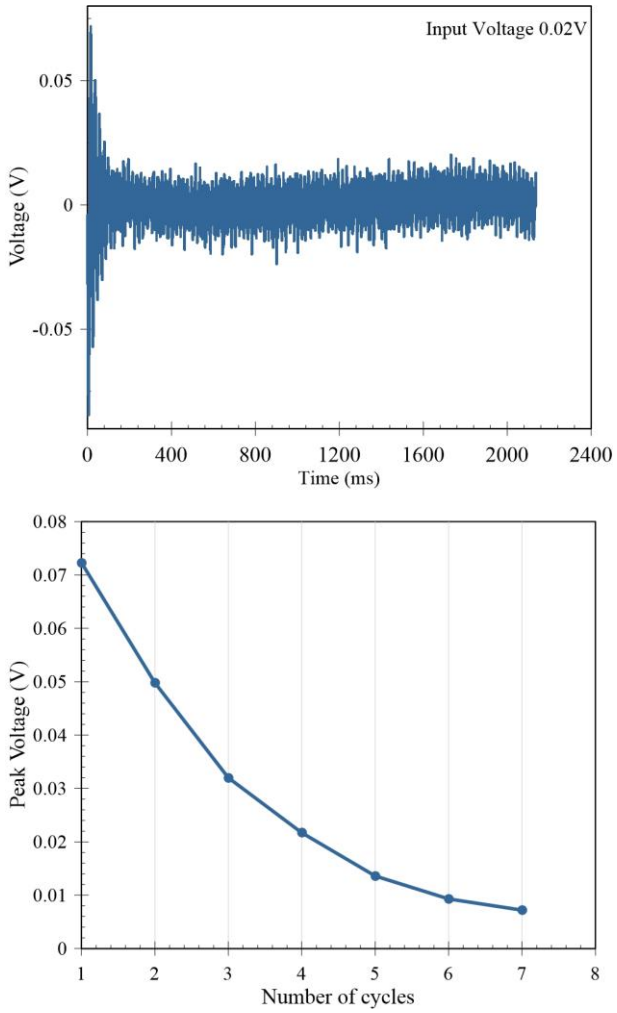

Fig. 5 A common example of free vibration decay in flexural mode

vibration while precisely measuring the vibration amplitude (shown in Fig. 5) and resonance frequency (Dammala 2019). This study employed RCT at confining pressures (σ_c) at 50, 100, 150 and 200 kPa to evaluate the dynamic behavior of well-graded sand with silt.

4.1.1 Shear modulus vs. Shear strain

Fig. 6 illustrates the relationship between shear modulus (G) and shear strain under varying confining pressures. The results show that as the amplitude of shear strain increases, the shear modulus decreases, indicating a reduction in soil stiffness. At higher strain levels, the influence of confining pressure on material stiffness diminishes, reflecting the non-linear behavior of soil under dynamic loading conditions.

At lower strain levels, the results reveal a significant increase in shear modulus values, highlighting the critical role of confining pressure. Higher confining pressures promote denser grain packing, which enhances material stiffness and shear stiffness (Adari *et al.* 2023). This behavior is particularly relevant at greater depths, where the denser soil matrix contributes to larger dynamic G values.

These findings emphasize the critical role of confining pressure in influencing soil stiffness, particularly at low

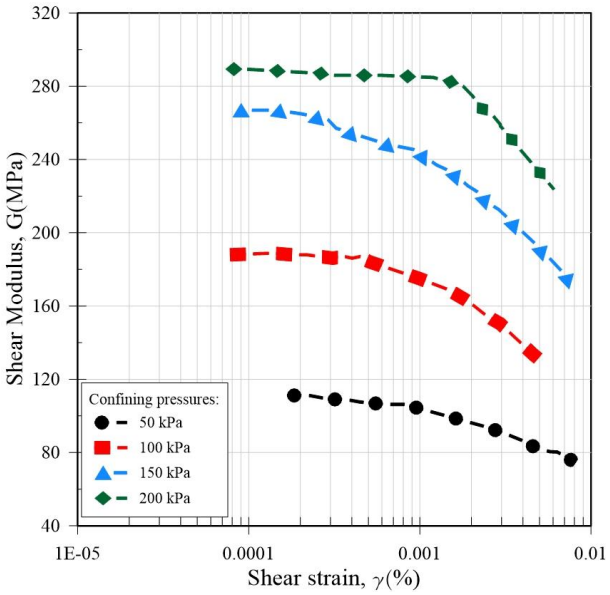

Fig. 6 Shear modulus vs. shear strain for different σ_c (for RC tests)

strain levels. Understanding this relationship is essential for geotechnical applications, including seismic hazard assessments, foundation design, and evaluating soil-structure interactions under dynamic loads.

4.1.2 Damping ratio vs. Shear strain

The damping ratio (D) of the well-graded sand with silt was computed using the free vibration decay method in accordance with ASTM standards (2015). The response of the soil sample was measured using an accelerometer mounted on the RC drive plate. During testing, the excitation was turned off, and the subsequent decay of free vibrations caused by sinusoidal stimulation was recorded.

The logarithmic decrement method was used to estimate the decay curve, where the slope of the best-fit line represents the logarithmic decrement. The algorithm utilized 10 vibration cycles to determine the damping ratio, as represented in Fig. 7 (GDS Resonant Column 2010).

The damping ratio (D) was calculated using the following equations:

$$D = \sqrt{\frac{\delta^2}{4\pi^2 + \delta^2}} \tag{5}$$

$$D = \frac{1}{2\pi n} \ln\left(\frac{Z_0}{Z_n}\right) \tag{6}$$

where, Z_0 is the vibration amplitude immediately after the excitation power is cut off, Z_n is the oscillation amplitude after the nth cycle, δ is the logarithmic decrement, and n is the number of cycles.

As shown in Fig. 7, the damping ratio increases with shear strain, following an upward concave trend. This is attributed to the higher energy dissipation associated with increased cyclic loading amplitudes (Adari *et al.* 2023).

Notably, the damping ratio is largely unaffected by

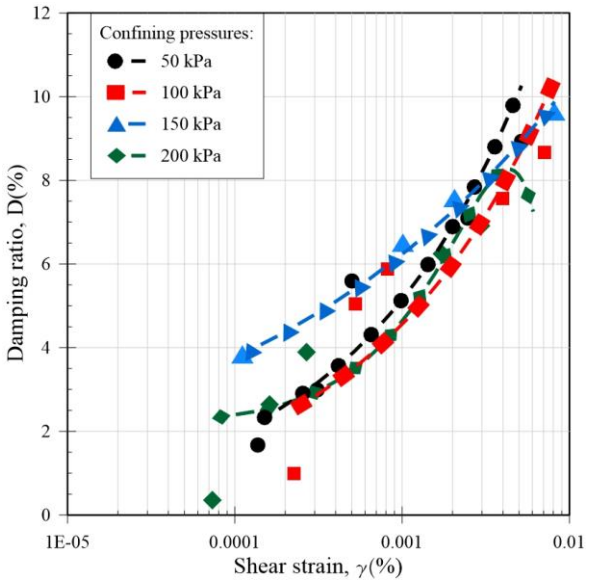

Fig. 7 Damping ratio vs. shear strain for different σ_c (for RC tests)

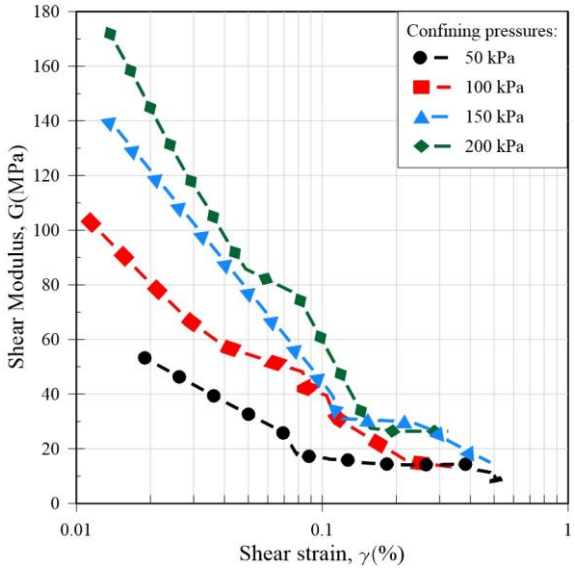

Fig. 8 Shear Modulus vs. Shear strain for different σ_c (for CTS tests)

variations in confining pressure across the measured strain range, indicating that the inherent material properties remain consistent. However, greater confining pressures are associated with a slight decrease in the damping ratio at higher strain levels, potentially due to enhanced particle interaction and reduced energy dissipation.

4.2 Cyclic Torsional Shear (CTS) testing

To investigate the impact of low-energy cyclic loading on the well-graded sand with silt sample, CTS tests were conducted using the same resonant column apparatus under a range of confining pressures (σ_c) from 50 kPa to 200 kPa. Each experiment was carried out sequentially. For the initial CTS tests, the coils were operated at the lowest voltage feasible, producing a strain amplitude of approximately 0.01% (Sakshi and Sebastian 2023). Subsequent experiments at each confining pressure progressively increased the excitation voltage to achieve a strain amplitude of 1%, covering a variety of strain amplitudes.

Unlike Resonant Column Testing (RCT), CTS testing focuses on hysteresis loops plotted on the $\tau - \gamma$ axis to enable the determination of to determine the shear modulus (G) and damping ratio (D) for each loading cycle. The calculations are based on the following equations

$$G = \frac{\tau_{pp}}{\gamma_{pp}} \tag{7}$$

$$D = \frac{1}{4\pi} \cdot \frac{\Delta W}{W} \tag{8}$$

where, ΔW represents the energy dissipated over the loading cycle, W denotes the stored elastic energy, and τ_{pp} and γ_{pp} correspond to the peak double-amplitude shear stress and strain, respectively (Facciorusso 2020).

4.2.1 Shear modulus vs. Shear strain

The relationship between shear modulus (G) and shear strain obtained from CTS test is illustrated in Fig. 8. At larger strains (greater than 0.1%), the influence of confining pressure (σ_c) on the shear modulus becomes negligible. Unlike RCT, CTS testing applies a slow, quasi-static load, allowing for strain amplitudes that exceed those of the RC tests.

The results indicate that the shear modulus values (G) pressures during the initial loading phases declined with an upward concave trend as strain values increased. This behavior underscores the progressive reduction in soil stiffness under higher strain amplitudes, regardless of confining pressure.

4.2.2 Damping ratio vs. Shear strain

The damping ratios (D) derived from CTS analysis demonstrate a consistent increase with higher shear strain magnitudes. This trend, illustrated in Fig. 9, shows a concave upward behavior at smaller strain levels, which gradually becomes less pronounced at larger strains. Interestingly, as σ_c increases, the damping ratios (D) tend to decrease slightly, particularly at higher strain amplitudes. Beyond a strain level of approximately 0.1%, the effect of confining pressure on the damping ratio diminishes. This behavior reflects the reduced energy dissipation capacity of well-graded sand with silt under higher confining pressures, where particle interaction becomes more constrained (Adari *et al.* 2023).

4.2.3 Effect of shearing strain

Fig. 10 illustrates the response of well-graded sand with silt to cyclic torsional shear (CTS) testing at a confining pressure of 150 kPa, evaluated across varying numbers of loading cycles: (a) N=1, (b) N=10, (c) N=100, and (d) N=1000. The values $\Delta\gamma$ = 0.06, 0.1, 0.16, and 0.22% represent the cyclic shear strain amplitudes applied during testing. These shear strain levels correspond to different stress amplitudes, affecting the evolution of soil behavior with increasing cycles.

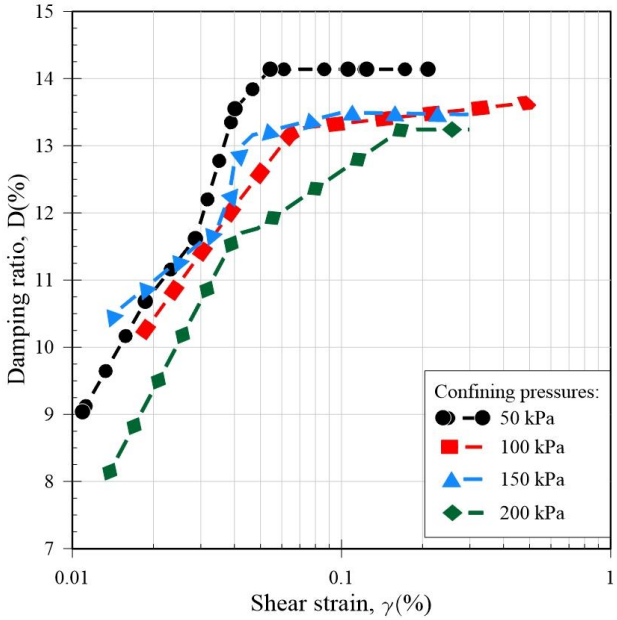

Fig. 9 Damping ratio vs. Shear strain for different σ_c (for CTS tests)

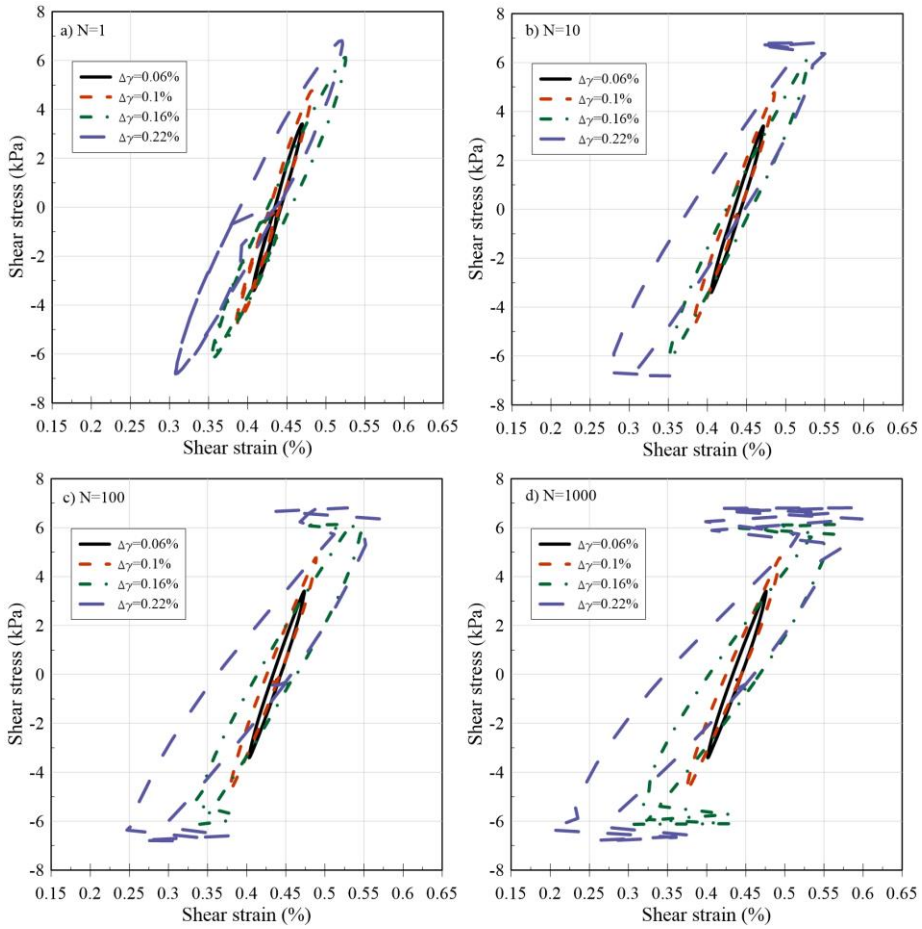

Fig. 10 Hysteretic response of well-graded sand with silt at loading cycles of an a) N=1, b) N=10, c) N=100, and d) N=1000

At low strain amplitudes ($\Delta\gamma$ = 0.06%), the soil exhibits a nearly elastic response, with minimal changes in loop shape even after 1000 cycles. However, at higher strain amplitudes ($\Delta\gamma$ = 0.22%), the loops show significant expansion and asymmetry, indicating increased deformation, particle rearrangement, and potential dilation effects. This transition is

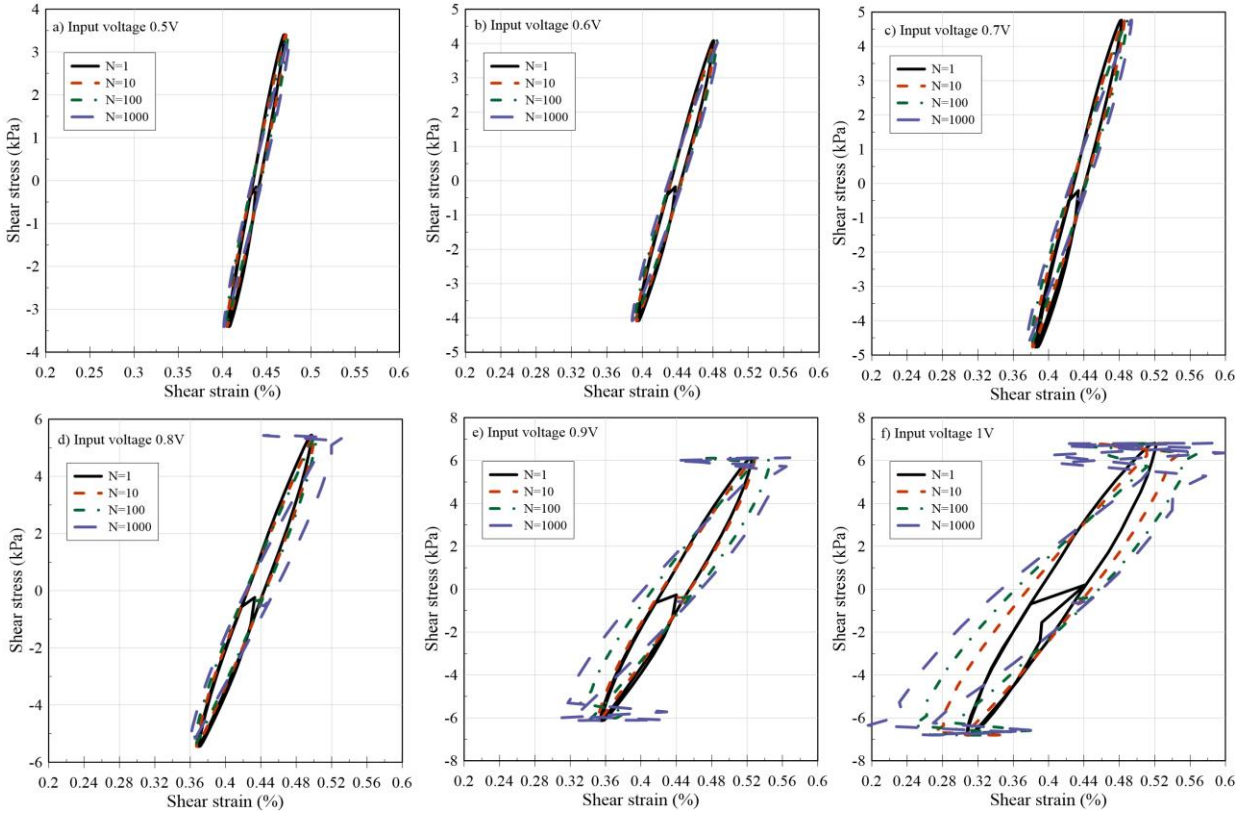

Fig. 11 Hysteretic response of well-graded sand with silt at a) 0.5V, b) 0.6V, c) 0.7V, d) 0.8V, e) 0.9V, f) 1V input voltages

reflected in the progressive softening of the soil, as seen in the gradual reduction of loop stiffness with increasing cycles (Adari *et al.* 2023).

The transition from convex (oval-shaped structure) to concave hysteresis loops reflects the soil's progression from a stable, bonded structure to a state of particle readjustment and dilative behavior. In the early cycles (N=1 and N=10), the loops maintain a more compact and stiff shape, whereas at N=100 and N=1000, they evolve into a more concave and elongated form. This shift highlights the strain-dependent nonlinearity of the soil, where cyclic loading leads to progressive degradation in stiffness and increased energy dissipation.

A strong correlation is observed between Figs. 8 and 10, as Fig. 8 presents the degradation of shear modulus (G) with increasing shear strain, while Fig. 10 captures the hysteresis loops of the same soil under different strain amplitudes and loading cycles at 150 kPa confining pressure. The shear modulus values in Fig. 8 were obtained from CTS tests conducted at progressively increasing strain amplitudes, including the values depicted in Fig. 10.

The observed trends in loop expansion and modulus reduction confirm the strain-dependent softening behavior of the soil, reinforcing its relevance in seismic analysis and foundation design under cyclic loading conditions.

4.2.4 Effect of loading cycles

Fig. 11 presents the hysteretic behavior of well-graded sand with silt under CTS testing at a confining pressure of 150 kPa, observed at different input voltages: (a) 0.5V, (b) 0.6V, (c) 0.7V, (d) 0.8V, (e) 0.9V, and (f) 1V. The shear stress-strain loops show a notable upward trend, with steeper slopes during the initial cycles as input voltage increases. As voltage and strain levels rise, the loops expand asymmetrically, reflecting a gradual transition toward more nonlinear soil behavior. This asymmetry becomes particularly pronounced at higher voltages (0.8V, 0.9V, and 1V), indicating significant changes in the soil's internal structure under increased shear stresses and larger cycle numbers. The expansion and asymmetry of the loops suggest that higher strain amplitudes induce particle rearrangement, leading to a transition from compact to more dispersed soil configurations.

Compared to Fig. 10, where loop evolution is driven by increasing loading cycles (N) at a constant strain amplitude, Fig. 11 focuses on how the soil responds to increasing strain amplitudes due to higher input voltages. In Fig. 10, the loops gradually change shape with increasing N, transitioning from convex to concave as strain accumulates over repeated cycles. This shift reflects progressive deformation and a loss of initial stiffness. In contrast, Fig. 11 demonstrates how higher input voltages immediately lead to wider and more asymmetric loops, signifying nonlinear behavior and greater energy dissipation.

The observed asymmetric hysteresis loops align with previous studies on sandy soils, which report that high-strain dynamic conditions, such as those induced by elevated input voltages, lead to complex, nonlinear soil

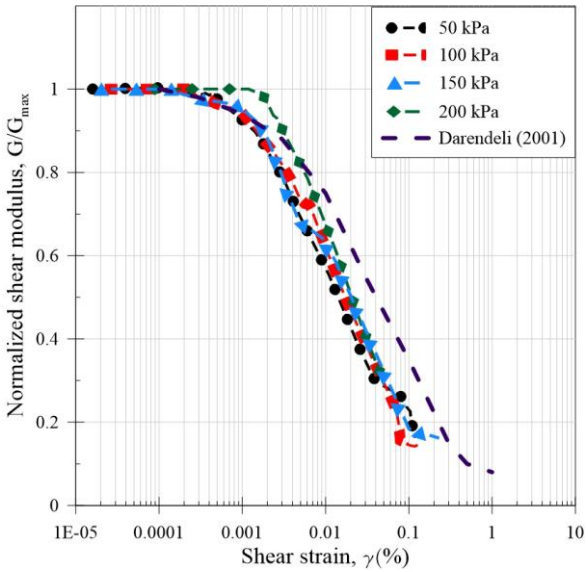

Fig. 12 G/G_{max} vs. γ for well-graded sand with silt

responses with distinctive stress-strain paths (Kumar *et. al* 2017). The increasing asymmetry and loop expansion with strain demonstrate how repeated high-strain cycles contribute to greater deformation and a potential reduction in stability.

The asymmetry of loops refers to deviations from the ideal elliptical shape, where stress-strain behavior becomes uneven due to strain localization and energy dissipation. These characteristics underscore the importance of accurately simulating soil behavior under high-strain conditions, where dynamic properties like stiffness and damping require careful evaluation. Understanding these behaviors is essential for geotechnical applications involving high-strain dynamic loading, such as seismic assessments and the design of foundations for critical infrastructure.

4.3 Normalized shear modulus (G/G_{max})

Fig. 12 illustrates the relationship between the normalized shear modulus (G/G_{max}) versus shear strain (γ) for well-graded sand with silt tested under confining pressures of 50 kPa, 100 kPa, 150 kPa, and 200 kPa. The data is split into two distinct regions based on the testing method employed: the resonant column (RC) test, which captures the low-strain range from 10^{-5} % to 0.01%, and the cyclic torsional shear (CTS) test, which extends beyond 0.01%. The RC test provides critical insights into soil behavior in the low-strain range, where stiffness remains relatively high, while the CTS test reveals the progressive reduction in stiffness at higher strain levels.

In the low-strain range (up to about 0.001%), minimal variation in normalized shear modulus across different confining pressures. This consistency reflects the strong retention of stiffness within the elastic response range of the well-graded sand with silt. However, as strain increases into the intermediate range (from 0.001% to 0.1%), a gradual reduction in G/G_{max} becomes evident, signaling the onset of soil softening.

At higher strain levels (beyond 0.1%), the reduction in G/G_{max} becomes more pronounced, with modulus values showing a sharp decrease. This trend aligns closely with the reference curve proposed by Darendeli (2001) for well-graded sand with silt, which serves as a benchmark for strain-dependent stiffness behavior. The convergence of the experimental data with the Darendeli model indicates that the model provides an accurate representation of the stiffness degradation of well-graded sand with silt under varying confining pressures.

This comparison emphasizes the transition of well-graded sand with silt from an initially elastic to a more plastic response as strain levels increase. By capturing these transitions, the study provides a comprehensive understanding of how well-graded sand with silt stiffness evolves across a wide range of strain levels, offering valuable insights for geotechnical applications such as seismic design and foundation stability assessments.

5. Conclusions

The combined findings from the Resonant Column (RC) and Cyclic Torsional Shear (CTS) tests provide valuable insights into the strain-dependent behavior of well-graded sand with silt under varying confining pressures. These results contribute to a deeper understanding of the mechanical properties of well-graded sand with silt and its behavior under dynamic loading conditions.

- The RC test data reveal that well-graded sand with silt maintains high stiffness at very low strains, with minimal reduction in shear modulus across different confining pressures. This indicates that well-graded sand with silt retains its elasticity well in shallow or low-strain environments.
- As strain levels increase, a gradual reduction in shear modulus is observed, signaling the onset of material softening. This trend, consistent across confining pressures, highlights the diminishing elasticity of well-graded sand with silt as strain increases.
- The CTS test results demonstrate a more pronounced decrease in stiffness at higher strain levels, aligning closely with the Darendeli (2001) model for well-graded sand with silt. This agreement validates the model's reliability in accurately capturing high-strain behavior for this soil type.
- Hysteresis loops observed during CTS testing transition from convex to concave shapes with increased loading cycles. This transformation reflects internal structural changes, including particle arrangement and increased void spaces, which contribute to a loss of stability and heightened deformation potential under cyclic loading.
- The results underscore the importance of considering strain levels and confining pressures when evaluating the mechanical properties of well-graded sand with silt. The strong correlation with predictive models like Darendeli (2001) supports their applicability in engineering practices, particularly in seismic hazard assessments and foundation design, where understanding the effects of cyclic loading is critical.

Overall, the study enhances our understanding of the dynamic soil properties of Astana's well-graded sand with silt, offering valuable insights for seismic hazard assessment and infrastructure development in the region. To further build on these findings and improve urban resilience in high-risk areas, additional investigations are necessary to refine predictive models and expand their applicability under varied geotechnical conditions. Future research should explore the application of these findings to other soil types in Kazakhstan, such as clay and gravel, as well as under diverse environmental conditions, including varying moisture levels and temperature fluctuations, to broaden the scope of their practical utility.

Acknowledgments

This research was funded by the Ministry of Education and Science (MES) Grant No. AP19675456, and Nazarbayev University, Collaborative Research Project (CRP) Grant No. 111024CRP2011. Any thoughts, conclusions, results, or suggestions made in this content belong to the author or authors and may not represent the viewpoints of Nazarbayev University.

References

Abdialim, S., Paiyz, N., Kim, J., Ku, T. and Moon, S.W.. (2024), "Evaluation of the dynamic soil characteristics of loam soils from MASW in Kazakhstan", *Proceedings of the 8th International Conference on Earthquake Geotechnical Engineering*, May 7-10, 2024, Osaka, Japan. https://doi.org/10.3208/jgssp.v10.OS-13-01.

Abdialim, S., Tuzelbayev, D., Shokbarov, Y., Khomyakov, V., Kim, J., Ku, T. and Moon, S.W. (2024), "Site characterization with surface waves in Kazakhstan", *Proceedings of the 7th International Conference on Geotechnical and Geophysical Site Characterization*, June 18-21, 2024, Barcelona, Spain.

Adari, S., Dammala, P.K., and Adapa, M.K. (2023), "Comprehensive dynamic characterization of two cohesive soils of northeastern India for effective stress–based seismic ground response analysis", *Arabian J. Geosci.*, **16**(10), 577. https://doi.org/10.1007/s12517-023-11651-3

ASTM D4015–15 (2015), "Standard test methods for modulus and damping of soils by resonant-column method", *ASTM International*, West Conshohocken, PA.

Clayton, C.R.I., Priest, J.A. and Bui, M. (2009), "The Stokoe resonant column apparatus: Effects of stiffness, mass, and specimen fixity", *Geotechnique*, **59**(5), 429-437. https://doi.org/10.1680/geot.2007.00096.

Cui, Z.D., Zhang, L.J. and Zhan, Z.X. (2023), "Dynamic shear modulus and damping ratio of saturated soft clay under the seismic loading", *Geomech. Eng.*, **32**(4), 411-426. https://doi.org/10.12989/gae.2023.32.4.411.

Dammala, P. (2019), "Dynamic characterisation of soils and seismic analysis of deep foundations", *Indian Institute of Technology Guwahati*.

Facciorusso, J. (2020), "An archive of data from resonant column and cyclic torsional shear tests performed on Italian clays", *Earthq. Spectra*, **37**(1), 545-562.

Flores-Guzmán, M., Ovando-Shelley, E. and Valle-Molina, C. (2014), "Small-strain dynamic characterization of clayey soil from the Texcoco Lake, Mexico", *Soil Dyn. Earthq. Eng.*, **63**, 1-7.

Güler, E. and Afacan, K. B. (2023), "Combined resonant column and cyclic triaxial tests to estimate the dynamic behavior of undisturbed saturated clayey soils of Adapazari, Turkey", *Geomech. Eng.*, **33**(3), 243-259. https://doi.org/10.12989/gae.2023.33.3.243.

Hardin, B.O. and Music, J. (1965), "Apparatus for vibration of soil specimens during the triaxial test", *Instruments and Apparatus for Soil and Rock Mechanics*, **392**, ASTM STP, 55-74.

Hardin, O. (1970), "Suggested methods of test for shear modulus and damping of soils by the resonant column", *ASTM International*.

Iida, K. (1938), "The velocity of elastic waves in sands", *Bulletin of Earthquake Engineering Research Institute*, Tokyo Imperial University, 131-144.

Khoshemehr, G.A. and Bahadori, H. (2023), "Investigating the dynamic response of deep soil mixing and gravel drain columns in the liquefiable layer with different thickness", *Geomech. Eng.*, **34**(6), 665-681. https://doi.org/10.12989/gae.2023.34.6.665.

Kumar, S.S., Krishna, A.M. and Dey, A. (2017), "Evaluation of dynamic properties of sandy soil at high cyclic strains", *Soil Dyn. Earthq. Eng.*, **99**, 157-167. https://doi.org/10.1016/j.soildyn.2017.05.016.

Kumar, S., Choudhary, S.S. and Burman, A. (2024), "Machine induced dynamic field responses of group pile with different pile arrangements", *Int. J. Geo-Eng.*, **15**(1). https://doi.org/10.1186/s40703-024-00207-3.

Mahinroosta, R. and Oshtaghi, V. (2021), "The effect of particle shape on the deformation and stress reduction of a gravel soil due to wetting", *Scientific Reports*, **11**(1). https://doi.org/10.1038/s41598-021-95731-y.

Moon, S.W., Mukhtarkhan, D., Khamitov, R., Abdialim, S., Khomyakov, Y., Kim, J. and Ku, T. (2024), "Liquefaction assessment using surface waves in Kazakhstan", *Proceedings of the 18th World Conference on Earthquake Engineering (WCEE2024)*, June 30 – July 5, 2024, Milan, Italy.

Nguyen, A.D., Nguyen, V.T. and Kim, Y.S. (2023), "Finite element analysis on dynamic behavior of sheet pile quay wall dredged and improved seaside subsoil using cement deep mixing", *Int. J. Geo-Eng.*, **14**(1). https://doi.org/10.1186/s40703-023-00186-x.

Rashid, M.S., Zhang, D., Moon, S.W., Sarkulova, D., Shokbarov, Y. and Kim, J. (2023), "Macro-seismic assessment for residential buildings constructed in the Soviet Union era in Almaty, Kazakhstan", *Buildings*, **13**(4), 1053.

Rohilla, S., and Sebastian, R. (2023), "Resonant column and cyclic torsional shear tests on Sutlej river sand subjected to the seismicity of Himalayan and Shivalik hill ranges: A case study", *Soil Dyn. Earthq. Eng.*, **166**, 107766. https://doi.org/10.1016/j.soildyn.2023.107766.

Sas, W., Gabryś, K. and Szymański, A. (2017), "Experimental studies of dynamic properties of Quaternary clayey soils", *Soil Dyn. Earthq. Eng.*, **95**, 29-39. https://doi.org/10.1016/j.soildyn.2017.01.031.

Shinde, N.S. and Kumar, J. (2021), "Calibration exercise of fixed-free resonant column apparatus", (Eds., T.G. Sitharam, S.V. Dinesh, R. Jakka), *Soil Dynamics*, Lecture Notes in Civil Engineering, vol 119, Springer, Singapore. https://doi.org/10.1007/978-981-33-4001-5_4.

Szilvágyi, Z. (2018), "Dynamic soil properties of Danube sands", PhD thesis.

Zhanabayeva, A., Moon, S.W., Ocheme, J.I., Yeraly, S., Khomyakov, V.A., Kim, J. and Satyanaga, A. (2023), "Comparative analysis of seismic design codes adhering to the Kazakhstani and European approaches", *Sustainability*, **15**, 615. https://doi.org/10.3390/su15010615.